Suppression of Error-Field-Induced Magnetic Islands by Alfvén Resonance Effect in Rotating Plasmas

M. Furukawa[1)] and L. -J. Zheng[2)]

[1)] Grad. Sch. Frontier Sci., Univ. Tokyo, Kashiwa, Chiba 277-8561, Japan
[2)] Institute for Fusion Studies, Univ. Texas at Austin, Austin, TX 78712, USA

E-mail: furukawa@k.u-tokyo.ac.jp

Abstract: Theory of error-field-induced magnetic islands is developed with the inclusion of the Alfvén resonance effect for rotating plasmas in cylinder model. Our results show that the Alfvén resonance effect changes the tearing mode parameter (Δ') dramatically and consequently plays a crucial role in the rotation suppression of the error-field-induced magnetic islands. Especially, for the small-error-field case, the inclusion of the Alfvén resonance effect can lead to a complete rotation suppression of the magnetic islands induced by the error field. The presence of the Alfvén resonance effect causes also a significantly larger torque, which increases as the plasma rotation is increased.

1. Introduction

Stabilization of the resistive-wall modes (RWMs) [1] is one of the crucial issues to sustain high-performance tokamak discharges. The plasma rotation stabilization of RWMs has been confirmed both experimentally [2–4] and theoretically [5–10]. Extensive experimental efforts have been made to measure the so-called critical rotation frequency for suppressing RWMs. With the error field braking of the plasma rotation, the critical rotation frequency is measured to be around a few percent of the shear Alfvén frequency [2]. Due to the evolution of the experimental facilities, both JT-60U and DIII-D have conducted the counter neutral beam braking experiments to measure the critical rotation frequency. Surprisingly, it is found that the critical rotation frequency is actually a few thousandth of the shear Alfvén frequency [3, 4]. This big drop in the critical rotation frequency by switching from the error-field-braking experiments to counter neutral beam braking ones indicates that the error field should play a critical role in deteriorating the plasma confinement.

Theoretically, the presence of the error field causes the breaking of the toroidal symmetry. Consequently, the magnetic islands can be created at the mode-resonant surfaces [11]. As shown for example in Refs. [12] and [13], the static error-field-induced island can give rise to a significant toroidal torque that brakes the plasma rotation. The balance between the magnetic-island-induced and the viscous torques has been shown to form the so-called forbidden band [12, 14]. Subsequently, the rotation bifurcation based on the forbidden band has been used to explain the current experimental observation of the low critical plasma rotation [15, 16]. Such a model predicts that the plasma rotation at the critical point is on the order of half of the unperturbed rotation.

However, the present model for the magnetic-island-induced torque has not taken into account the Alfvén resonance effect. The Alfvén resonance effect together with the Reynolds stress is investigated in the ideal plasma in Ref. [17]. The Alfvén resonance effects on the magnetic island formation were studied in Ref. [18] by using numerical simulation in a slab geometry. Subsequently, it is further investigated analytically in Ref. [19]. The linear theory of the Alfvén resonance effect on the island formation is also investigated in Ref. [12]. In this paper, we extend

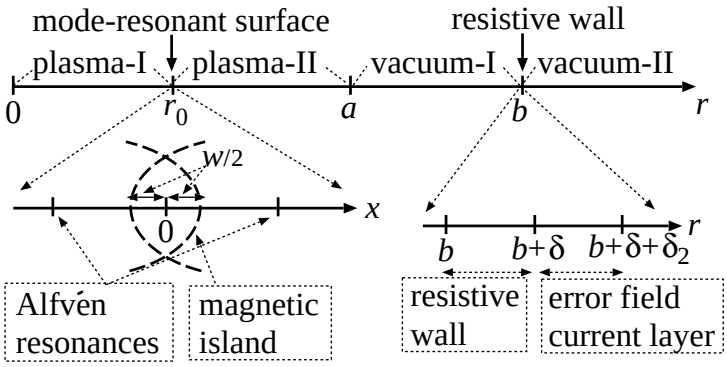

FIG. 1. Schematic picture of the geometry.

the nonlinear theory of Ref. [12] to include the Alfvén resonance effect. As explained below, we found a new stationary state of non-rotating islands where the convection term balances with the Δ' term. We discovered a new mechanism by which the islands can be eliminated due to the change in the so-called tearing modes parameter Δ' caused by the Alfvén resonances. As compared with the analytical approach in Ref. [19], our numerical investigation allows us to consider the dependence of Δ' on the finite island width.

Physically, the Doppler shift due to the plasma rotation breaks the single resonance at the mode-resonant surface into the twin resonances. For the case with the separation of the twin Alfvén resonances being larger than the island width, these twin Alfvén resonances can change dramatically the way in which the magnetic perturbations approach to the mode rational surface and consequently the pattern in which the magnetic islands are formed. This intuitive consideration has motivated us to further investigate the Alfvén resonance effect on the formation of magnetic islands. As expected, it is found that the Alfvén resonance effect is a crucial effect in determining both the island formation and the toroidal torque that brakes the plasma rotation.

The present paper is organized as follows. In Sec. 2., Theory for error-field-induced magnetic islands in the presence of the Alfvén resonances is developed; In Sec. 3., the numerical results is shown and the Alfvén resonance effect on the error-field-induced islands is addressed; In Sec. 4. conclusions and discussion are given.

2. Theory for error-field-induced magnetic islands with the Alfvén resonance effect taken into account

In this section, we develop a theory for the error-field-induced magnetic islands. In difference from the existing theories, the Alfvén resonance effect is taken into account in our current theory. For simplicity, we use the cylinder model and consider only the case with the separation of the twin Alfvén resonances being larger than the island width. For typical parameters of large tokamaks, a plasma rotation velocity with several percents of Alfvén velocity leads the separation of Alfvén resonances of order of centimeter. This can be much larger than the magnetic island size, especially when the island size is reduced by the plasma rotation. The system is described as follows: The plasma column is surrounded by the vacuum region, the resistive wall is located in the vacuum region. The resistive wall is assumed to be thin. Just outside the resistive wall, a thin error field current layer is present. The schematic view of the geometry is shown in Fig. 1. Our derivation consists of mainly two parts: (i) constructing the independent solutions in the outer regions and (ii) matching the independent solutions across the resonance layers, wall, and the error-filed-current layer.

2.1. Construction of the independent solutions

We first construct the independent solutions in various outer regions, where the time dependence and dissipative effects can be neglected. These independent solutions will be connected by the appropriate matching conditions derived in the next subsection. We focus ourselves on considering the current-driven instabilities and therefore the finite plasma beta effect is neglected.

Vacuum-II region: Let us first consider Vacuum-II region. In the vacuum region, we use a scalar potential ψ to express the perturbed magnetic field as $\tilde{\mathbf{B}} = \nabla\psi$. Then ψ satisfies the Laplace equation since $\nabla \cdot \tilde{\mathbf{B}} = 0$. We assume that ψ has the spacial dependence as $\mathrm{e}^{\mathrm{i}(m\theta-(n/R_0)z)}$, where the cylindrical coordinate system (r, θ, z) is used. Since the Laplace equation is the second-order ordinary differential equation, it has two independent solutions. The boundary condition, $\psi \to 0$ at $r \to \infty$, selects one of the independent solutions as

$$\psi^{\mathrm{vII}}(r) = (r/b)^{-m}, \tag{1}$$

where the superscript "vII" denotes "vacuum-II region". Similar notations will be used in the following. Then, the scalar potential in the vacuum-II region is expressed as

$$\psi(r) = c^{\mathrm{vII}}\psi^{\mathrm{vII}}(r). \tag{2}$$

Vacuum-I region: In the Vacuum-I region, we have two independent solutions. Here we adopt

$$\psi_1^{\mathrm{vI}}(r) = [(r/b)^m + (r/b)^{-m}]/2, \qquad \psi_2^{\mathrm{vI}}(r) = (r/b)^{-m}, \tag{3}$$

where $\psi_2^{\mathrm{vI}}(r)$ connects smoothly onto $\psi^{\mathrm{vII}}(r)$. The solutions $\psi_1^{\mathrm{vI}}(r)$ and $\psi_2^{\mathrm{vI}}(r)$ correspond to an ideal-wall and no-wall solutions, respectively. By using these independent solutions, the scalar potential in the vacuum-I region is expressed as

$$\psi(r) = c_1^{\mathrm{vI}}\psi_1^{\mathrm{vI}}(r) + c_2^{\mathrm{vI}}\psi_2^{\mathrm{vI}}(r). \tag{4}$$

Plasma-II region: In the Plasma-II region, we solve the following equation [20]:

$$\frac{\mathrm{d}}{\mathrm{d}r}\left[(\rho n^2\Omega_0^2 - F^2)r\frac{\mathrm{d}}{\mathrm{d}r}(r\xi)\right] - \left[m^2(\rho n^2\Omega_0^2 - F^2) - r\frac{\mathrm{d}F^2}{\mathrm{d}r}\right]\xi = 0, \tag{5}$$

where ξ is the radial displacement of the plasma, ρ is the equilibrium mass density, Ω_0 is the equilibrium toroidal rotation frequency, F is defined as $F := \mathbf{k} \cdot \mathbf{B}$ where $\mathbf{k} := m\nabla\theta - (n/R_0)\nabla z$ is the wave-number vector, m and n are the poloidal and toroidal mode numbers, respectively, and R_0 is the plasma major radius. The effect of rotation is negligible in almost whole region except for the narrow layer around the mode-resonant surface where $F = 0$. In the narrow layer, the rotation frequency can be assumed constant. Therefore, it is sufficient to introduce constant Ω_0 in Eq. (5). The mass density ρ is also assumed constant for simplicity. It is straightforward to include the spatial dependence of Ω and ρ. In integrating Eq. (5) from the plasma edge $r = a$ to the edge of the magnetic island $r = r_0 + w/2$, the Alfvén singularity at the position with $F^2 - \rho(n\Omega_0)^2 = 0$ is avoided by replacing $n\Omega_0$ by $n\Omega_0 + \mathrm{i}\,\gamma$ with $0 < \gamma \ll n\Omega_0$ [10]. Equation (5) is the second-order ordinary differential equation, and thus we have two independent solutions; $\xi_1^{\mathrm{pII}}(r)$ and $\xi_2^{\mathrm{pII}}(r)$. By using $\psi_1^{\mathrm{vI}}(r)$ and $\psi_2^{\mathrm{vI}}(r)$ as well as the continuity of perturbed magnetic field and total pressure at the plasma edge [1], we can obtain boundary conditions for $\xi_1^{\mathrm{pII}}(r)$ and

$\xi_2^{\mathrm{pII}}(r)$ so that they smoothly connect to ideal-wall and no-wall solutions in the vacuum region, respectively. Then the plasma displacement $\xi(r)$ is expressed as

$$\xi(r) = c_1^{\mathrm{pII}}\xi_1^{\mathrm{pII}}(r) + c_2^{\mathrm{pII}}\xi_2^{\mathrm{pII}}(r), \tag{6}$$

where c_1^{pII} and c_2^{pII} becomes identical to c_1^{vI} and c_2^{vI}, respectively.

Plasma-I region: Finally, in the Plasma-I region, we also solve Eq. (5) from the magnetic axis $r = 0$ to the edge of the magnetic island $r = r_0 - w/2$. Since ξ must not diverge at $r = 0$, one of the two solutions is dropped, and we adopt the other as the independent solution; $\xi^{\mathrm{pI}}(r)$. Then, we express the plasma displacement in this region as

$$\xi(r) = c^{\mathrm{pI}}\xi^{\mathrm{pI}}(r). \tag{7}$$

2.2. Matching conditions and the magnetic island equation

Across magnetic island chain: The radial component of the perturbed magnetic field is expressed by $\tilde{B}_r = \mathbf{B}\cdot\nabla\xi = \mathrm{i}F\xi$. By using linear approximation of F just outside the magnetic islands, we have

$$\tilde{B}_r = -\frac{\mathrm{i}nB_zS_0}{R_0r_0}x\xi, \tag{8}$$

where $x := r - r_0$, B_z is the equilibrium toroidal magnetic field and S_0 is the magnetic shear $S := r(\mathrm{d}q/\mathrm{d}r)/q$ at the rational surface. The safety factor is denoted by q. One of the matching conditions is the continuity of $\tilde{B}_r$ across the island, which can be expressed as $-\xi(-w/2) = \xi(w/2)$ where the suffix means $x = \pm w/2$. If we normalize $\xi_1^{\mathrm{pII}}(r)$ and $\xi_2^{\mathrm{pII}}(r)$ such that $-\xi^{\mathrm{pI}}(-w/2) = \xi_1^{\mathrm{pII}}(w/2) = \xi_2^{\mathrm{pII}}(w/2)$, we obtain

$$c^{\mathrm{pI}} = c_1^{\mathrm{pII}} + c_2^{\mathrm{pII}}. \tag{9}$$

It is noted that $c^{\mathrm{pI}} = c_1^{\mathrm{pII}}$ for the ideal wall case, whereas $c^{\mathrm{pI}} = c_2^{\mathrm{pII}}$ for the no wall case. The second condition is given by the r component of the induction equation:

$$\left(\frac{\partial}{\partial t} + \mathbf{v}\cdot\nabla\right)\tilde{B}_r = \mathbf{B}\cdot\nabla\tilde{v}_r + \frac{\eta}{\mu_0}\nabla^2\tilde{B}_r, \tag{10}$$

where η denotes the plasma resistivity and μ_0 is the vacuum permeability. Assuming that the island width is much smaller than the separation of the Alfvén resonances, $x \ll n\Omega_0$, we find that $\mathbf{B}\cdot\nabla\tilde{v}_r$ term can be neglected. It is noted that the magnetic shear S_0 is considered to be of order of unity. By considering stationary state with $\partial/\partial t = 0$ and by integrating Eq. (10) across the island, we obtain the modified Rutherford equation [21],

$$-\mathrm{i}\,n\alpha\Omega_0 w = \frac{\eta}{\mu_0}\Delta', \qquad \text{where} \qquad \Delta' := \frac{\partial\tilde{B}_r/\partial r\big|_{-w/2}^{w/2}}{\tilde{B}_r}. \tag{11}$$

Here, α denotes a ratio of the rotation frequency inside the islands to that outside them, which allows different plasma rotation frequency between inside and outside the islands. This equation describes a new stationary state of non-rotating islands where the convection term balances with the Δ' term. In the present paper, Δ' is generally a complex number, since we introduced the Alfvén resonances which make $\xi^{\mathrm{pI}}(r)$, $\xi_1^{\mathrm{pII}}(r)$ and $\xi_2^{\mathrm{pII}}(r)$ complex functions. By defining

$$\Delta'_\infty := \frac{4}{w} + \frac{\xi_2^{\mathrm{pII}\prime}(w/2) + \xi^{\mathrm{pI}\prime}(-w/2)}{-\xi^{\mathrm{pI}}(-w/2)}, \qquad \Delta'_b := \frac{4}{w} + \frac{\xi_1^{\mathrm{pII}\prime}(w/2) + \xi^{\mathrm{pI}\prime}(-w/2)}{-\xi^{\mathrm{pI}}(-w/2)}, \tag{12}$$

and by using $\tilde{B}_r = \mathrm{i}\, F\xi$ together with the expression for the island width $w = 4(rq|\tilde{B}_r|/mq'B_\theta)^{1/2}$ [20], we obtain

$$\Delta' = \Delta'_\infty - \frac{8\mathrm{i}\, w\xi^{\mathrm{pI}}(-w/2)c_1^{\mathrm{pII}}}{w^2}(\Delta'_\infty - \Delta'_b). \tag{13}$$

Across the plasma boundary: The boundary conditions across this interface has been already imposed through the choice of boundary conditions for $\xi_1^{\mathrm{pII}}(r)$ and $\xi_2^{\mathrm{pII}}(r)$. We obtained $c_1^{\mathrm{pII}} = c_1^{\mathrm{vI}}$ and $c_2^{\mathrm{pII}} = c_2^{\mathrm{vI}}$.

Across the resistive wall and error field current layer: Here we adopt a thin-shell approximation. One matching condition is the continuity of the radial magnetic field through vacuum-I to vacuum-II, which is imposed by setting $c_2^{\mathrm{vI}} = c^{\mathrm{vII}}$. One more condition across the resistive wall is given by the diffusion equation of the magnetic field. We integrate it across the resistive wall in the thin-shell approximation to obtain

$$\frac{\partial \tilde{B}_r}{\partial t} = -\frac{\eta_{\mathrm{w}}}{\mu_0 \delta} k_{0b}^2 (c_1^{\mathrm{vI}} \psi_1^{\mathrm{vI}}(b) + \psi_{\mathrm{err}}), \tag{14}$$

where η_{w} and δ are the resistivity and thickness of the wall, respectively, $k_{0b}^2 := (m/b)^2 + (n/R_0)^2$, and $\psi_{\mathrm{err}} = \left((\partial \tilde{B}_r/\partial r)_{b+\delta} - (\partial \tilde{B}_r/\partial r)_{b+\delta+\delta_2} \right) / k_{0b}^2$. The continuity of $\tilde{B}_r$ across the wall has been used. The parameter ψ_{err} is proportional to the jump of the tangential component of the magnetic field across the error-field-coil layer, and measures the strength of the error field. It is noted that $\psi_1^{\mathrm{vI}}(b) = -\xi^{\mathrm{pI}}(-w/2)/\xi_1^{\mathrm{pII}}(w/2)$. Assuming that $\partial/\partial t$ is so small that it can be neglected [3, 4], then we obtain

$$c_1^{\mathrm{vI}} \xi^{\mathrm{pI}}(-w/2)/\xi_1^{\mathrm{pII}}(w/2) = \psi_{\mathrm{err}}. \tag{15}$$

Magnetic island equation: By using the above matching conditions, we obtain $c_1^{\mathrm{pII}} = c_1^{\mathrm{vI}} = \psi_{\mathrm{err}} \xi_1^{\mathrm{pII}}(w/2)/\xi^{\mathrm{pI}}(-w/2)$, and therefore the island equation can be written as

$$-\mathrm{i}\, n\alpha\Omega_0 \frac{\mu_0}{\eta} w^3 = \Delta'_\infty w^2 - 8\mathrm{i}\, w\xi_1^{\mathrm{pII}}(w/2)\psi_{\mathrm{err}}(\Delta'_\infty - \Delta'_b). \tag{16}$$

By giving $|\psi_{\mathrm{err}}|$ and choosing the phase of the error field appropriately, we may find the solution w which must be restricted to be real and positive. Since Eq. (16) is a cubic equation for w, it is possible to obtain multiple solutions or bifurcation. Note that in our solution of Eq. (16) we have considered that Δ's depends on the island width w. The solution represents a new stationary state where the convection term balances with the Δ' term.

2.3. Toroidal torque

The perturbed magnetic field generates the torque on the plasma. By integrating the toroidal torque in an axisymmetric domain inside the error field current layer, we obtain [12, 22]

$$\tau_\varphi = -\mathrm{i}\, \pi^2 R_0^2 bk(\psi_{\mathrm{err}} \psi'^*(b) - \psi^*_{\mathrm{err}} \psi'(b)). \tag{17}$$

This torque has the same magnitude and the opposite direction as the total torque on the plasma.

3. Numerical results: Alfvén resonance effect on the error-field-induced islands

To show the Alfvén resonance effect on the error-field-induced islands, we solve Eq. (16) numerically for the island width, and calculate Eq. (17) for the torque. The quantities shown below are normalized by using the plasma minor radius a, the toroidal magnetic field B_z, and the Alfvén time $\tau_A := a/(B_z/\sqrt{\mu_0\rho})$. We adopt an equilibrium with toroidal current density profile as $j_t(r) = j_{t0}(1-r^2)$. The edge safety factor was chosen as $q_a = 2.2$. For this current density profile, we have $q_0 = q_a/2 = 1.1$. The rational surface of $m/n = 2/1$ locates at $r = 0.9487$, and thus we expect that $\Delta'_\infty - \Delta'_b$ has large value which may enhance the effect of the error field. We also assume that the resistive wall is located at $r = b = 1.1$. The resistivity parameter was chosen as $\eta/\alpha = 10^{-8}$.

It is interesting to show that the eigenfunction changes by the Alfvén resonances. Figure 2 shows the comparison of the real part of perturbed radial magnetic field $\tilde{B}_r$ between the cases without ($\Omega_0 = 0$) and with ($\Omega_0 = 10^{-2}$) the Alfvén resonance effect. The plotted data has its island width $w = 10^{-2}$. In the rotating case, we find the spiky behavior of $\tilde{B}_r$ at the Alfvén resonances $r = 0.9292$ and 0.9678. Although we do not show Δ' explicitly in this paper because of limited space, we may understand that Δ' is changed significantly. It is noted that we have performed benchmark of the numerical solution with the analytic solution [10] for the eigenfunction in the presence of the Alfvén resonance.

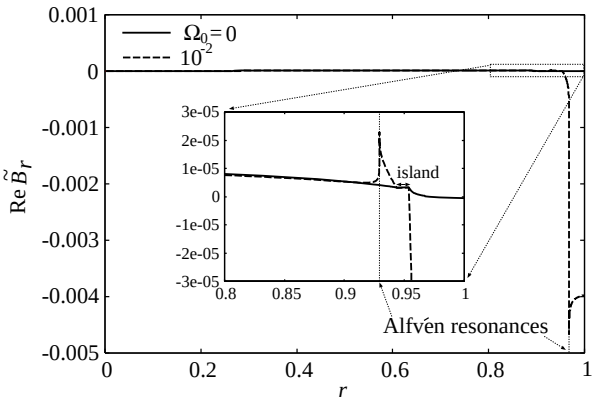

FIG. 2. Comparison of perturbed radial magnetic field between no-rotation and finite-rotation cases. Spiky behavior is observed at the Alfvén resonances.

Figure 3 shows the island width as a function of $|\psi_{\rm err}|$. In the figure, "w/ A.r. (w/o A.r.)" denotes data with (without) the Alfvén resonances: for "w/ A.r.", the plasma rotation effects are included as the Alfvén resonances in Eq. (5) as well as in the island equation (16), on the other hand, for "w/o A.r.", the plasma rotation effect is included only in Eq. (16) and Ω_0 is set to zero in Eq. (5). Without the Alfvén resonance effect, the island of width $w = 10^{-2}$ can be generated by $|\psi_{\rm err}|$ of order of 10^{-3}. On the other hand, with the Alfvén resonance effect included, significantly large $|\psi_{\rm err}|$ is needed to generate the islands. If we set $\Omega_0 = 0$ in both Eqs. (5) and (16), $w = 10^{-2}$ is obtained for $|\psi_{\rm err}| \sim 10^{-5}$. Figure 3 also shows the scaling change due to the inclusion of the Alfvén resonances. When the Alfvén resonances are included, the island width w is proportional to $|\psi_{\rm err}|^{4/7}$ approximately for relatively large w, whereas $|\psi_{\rm err}|^{1/3}$ in the absence of the Alfvén resonances [12]. For small w, slight change of $|\psi_{\rm err}|$ can lead to significant change of w in the presence of the Alfvén resonances.

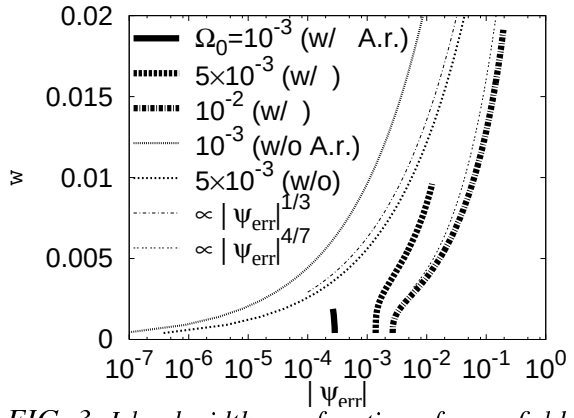

FIG. 3. Island width as a function of error field.

These observation can be seen alternatively from the figure of the island width versus the rotation frequency. Figure 4 shows the island width as a function of plasma rotation frequency. The

island width decreases as the rotation is increased. It is noted that "sep.Alf.res." in Fig. 4 denotes the separation of the Alfvén resonances. Since the island width is assumed to be smaller than the separation of the sep.Alf.res., we stopped the calculation of w if w is smaller than one half of the sep.Alf.res. Thus no data for "w/ A.r." is shown for the small w range. The island width is proportional to Ω_0^{-1} approximately for relatively large $|\psi_{\rm err}|$ in the presence of the Alfvén resonances, whereas $\Omega_0^{-1/3}$ in the absence of them [12]. These observations show that the rotation suppression of the error-field-induced magnetic islands is mainly through the induced Alfvén resonances. Most importantly, the Alfvén resonance can completely suppress the island formation by a small error field.

From the crucial role of the Alfvén resonances in suppressing the error-field-induced magnetic islands, one can expect that they should also bear a significant portion of the torque generation. Figure 5 shows the toroidal torque on the plasma, denoted by $-\tau_\varphi$, as a function of the plasma rotation frequency Ω_0. Two important conclusions can be drawn from our numerical results. First, the torque increases as the plasma rotation frequency, as well as the island width, increases. This is opposite to the case in which the Alfvén resonances are neglected. Second, one can also note that the torque magnitude becomes significantly larger by including the Alfvén resonances, as it should be in view of the big change in magnetic island width.

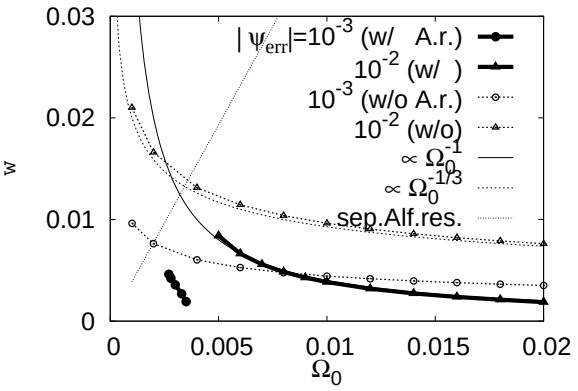

FIG. 4. Island width as a function of plasma toroidal rotation frequency.

4. Conclusions and discussion

In this paper, we developed a theory for static magnetic island induced by the error field with the Alfvén resonance effect taken into consideration for rotating plasmas in cylinder model. The theory applies to the case with magnetic islands lying inside the twin Alfvén resonances. This happens usually for relatively large plasma rotation. Even with this restriction, as mentioned at the beginning of Sec. 2., our parameters still cover a considerable parameter range that fits the current experiments. Several important conclusions have been found from the current investigation: (1) The Alfvén resonance effect changes dramatically the tearing mode parameter (Δ'); (2) The Alfvén resonance effect can enhance the rotation suppression of the error-field-induced magnetic islands. Especially, for the small-error-field case, the inclusion of the Alfvén resonance effect can lead to a complete rotation suppression of the magnetic islands induced by the error field; (3) The presence of the Alfvén resonance effect causes also a significantly larger torque and alters the pattern of the dependence of the torque versus the plasma rotation; (4) We also find that the scaling of the

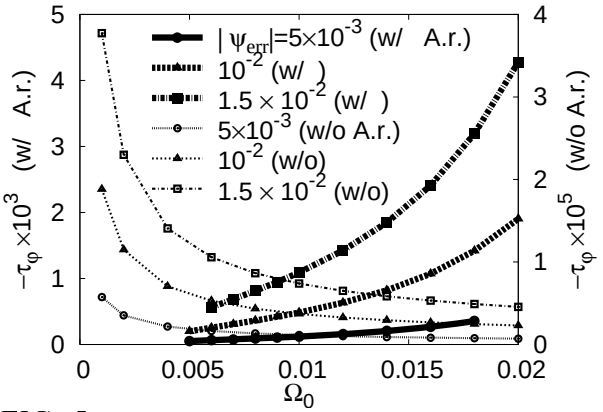

FIG. 5. Toroidal torque as a function of plasma toroidal rotation frequency.

island width versus the strength of the error field is changed from $|\psi_{\rm err}|^{1/3}$ to $|\psi_{\rm err}|^{4/7}$ due to the inclusion of the Alfvén resonances for relatively large w. For small w, slight change of $|\psi_{\rm err}|$ can lead to significant change of w in the presence of the Alfvén resonances. When $|\psi_{\rm err}|$ is relatively large, the island width w scales as Ω_0^{-1}.
In the present paper, we have developed a semi-analytic theory. By utilizing a nonlinear simulation code, we have obtained similar results as mentioned above. These will be reported in near future.

Acknowledgements: We would like to acknowledge helpful discussions with Dr. J. W. Van Dam. This work was supported by Joint Institute for Fusion Theory (JIFT) exchange program and partly by the Grant-in-Aid for Young Scientists (B) 19760595 (2007) from the Japan Society for the Promotion of Science(JSPS).

References

[1] J. P. Freidberg, *Ideal Magnetohydrodynamics* (Plenum Press, New York, 1987).
[2] E. J. Strait *et al.*, Phys. Rev. Lett. **74**, 2483 (1995).
[3] M. Takechi *et al.*, Phys. Rev. Lett. **98**, 055002 (2007).
[4] H. Reimerdes *et al.*, Phys. Rev. Lett. **98**, 055001 (2007).
[5] C. G. Gimblett, Nucl. Fusion **26**, 617 (1986).
[6] A. Bondeson and D. J. Ward, Phys. Rev. Lett. **72**, 2709 (1994).
[7] D. J. Ward and A. Bondeson, Phys. Plasmas **2**, 1570 (1995).
[8] R. Betti and J. P. Freidberg, Phys. Rev. Lett. **74**, 2949 (1995).
[9] J. M. Finn, Phys. Plasmas **2**, 198 (1995).
[10] L. -J. Zheng, M. Kotschenreuther, and M. S. Chu, Phys. Rev. Lett. **95**, 255003 (2005).
[11] A. H. Boozer, Phys. Fluids **27**, 2055 (1984).
[12] R. Fitzpatrick, Phys. Plasmas **5**, 3325 (1998).
[13] A. H. Boozer, Phys. Rev. Lett. **86**, 5059 (2001).
[14] D. A. Gates and T. C. Hender, Nucl. Fusion **36**, 273 (1996).
[15] E. J. Strait, A. M. Garofalo, G. L. Jackson *et al.*, Phys. Plasmas **14**, 056101 (2007).
[16] A. M. Garofalo, G. L. Jackson, R. J. La Haye *et al*, Nucl. Fusion **47**, 1121 (2007).
[17] J. B. Taylor, Phys. Rev. Lett. **91**, 115002 (2003).
[18] O. A. Hurricane, T. H. Jensen, A. B. Hassam, Phys. Plasmas **2**, 1976 (1995).
[19] A. H. Boozer, Phys. Plasmas **3**, 4620 (1996).
[20] J. Wesson, *Tokamaks* (Clarendon Press, Oxford, 2004).
[21] P. H. Rutherford, Phys. Fluids **16**, 1903 (1973).
[22] A. H. Boozer, Phys. Plasmas **10**, 1458 (2003).